# Run for your life – an integrated virtual tissue platform for incorporating exercise oncology into immunotherapy

Josua Aponte Serrano & Amit Hagar*

Department of Intelligent Systems engineering
School of Informatics
Indiana University Bloomington
Bloomington, IN 47405
USA

joaponte@iu.edu
hagara@iu.edu

* Corresponding Author
Orcid 0000-0002-7920-975X

**Abstract**

The purpose of this paper is to introduce a novel *in silico* platform for simulating early stage solid tumor growth and anti-tumor immune response. We present the model, test the sensitivity and robustness of its parameters, and calibrate it with clinical data from exercise oncology experiments which offer a natural biological backdrop for modulation of anti-tumor immune response. We then perform two virtual experiments with the model that demonstrate its usefulness in guiding pre-clinical and clinical studies of immunotherapy. The first virtual experiment describes the intricate dynamics in the tumor microenvironment between the tumor and the infiltrating immune cells. Such dynamics is difficult to probe during a pre-clinical study as it requires significant redundancy in lab animals and is prohibitively time and labor intensive. The result is a series of spatiotemporal snapshots of the tumor and its microenvironment that can serve as a platform to test mechanistic hypotheses on the role and dynamics of different immune cells in anti-tumor immune response. The second virtual experiment shows how dosage and frequency of immunotherapy drugs can be optimized based on the aerobic fitness of the patient, so that possible adverse side effects of the treatment can be minimized.

## 1. Introduction.

Computational modeling is playing increasingly important roles in advancing a system-level mechanistic understanding of complex interrelated biological processes such as the anti-tumor immune response. In silico simulations guide and underpin experimental and clinical efforts and can advance the knowledge discovery and accelerate therapeutic development at an unprecedented rate. Here we present a computational platform that can interrogate potential mechanisms underlying the effect of aerobic fitness on anti-tumor immune response. These effects, documented in pre-clinical [1,2] and clinical studies [3,4], furnish us with a natural backdrop for probing patient variability and as such may contribute to the personalization of immunotherapy by optimizing dosage and frequency of treatment and by reducing the risk of cardiotoxicity and other adverse side effects [5].

The model is based on the open source platform of CompuCell (CC3D) [6]. It is a 2D spatiotemporal representation of a cross section in the tumor microenvironment (TME), that allows visualization of the intricate dynamics between the tumor cells and the host immune response. Using data from pre-clinical and clinical studies, we have calibrated the model and estimated the range of the necessary parameters, performed sensitivity analysis, tested its robustness, and checked its biological significance by comparing its outcomes to data from clinical and pre-clinical literature. Once calibrated, the model was used to test several hypotheses in exercise oncology, and to perform a virtual experiment that probed the effect of aerobic fitness on cardiotoxicity as a potential adverse effect of immunotherapeutic drugs.

Our basics assumption is that aerobic fitness acts as a tumor suppressor through a systemic enhancement of anti-tumor immune response. This systemic effect is a result of metabolic and endocrinal modifications, which can be modulated with chronic exercise. While the exact mechanisms behind this effect are currently under investigation, documented pre-clinical experiments point at two potential candidates: (1) increased trafficking of NK cells into the TME, triggered by up-regulation of epinephrine [7,8] and (2) hypoxia-tolerant suppression of Treg recruitment into the TME which increases cytotoxic T lymphocytes (CTL) efficiency [9,10,11]. In the model presented here we chose to focus on candidate (2),[1] but the platform can be easily adjusted to incorporate candidate (1) or any other potential mechanism in the future.

## 2. Methods.

**2.1. Model description.** The model is a spatiotemporal representation of solid tumor progression in its early stage (T0 to T1) that includes key aspects of the interactions between tumor cells, the TME and the host immune response. In our model, tumor cells adopt four different phenotypes: “oxphos” (performing oxidative phosphorylation), “glycolytic” (elevated glycolysis), “necrotic” and “apoptotic”. Tumor cells grow, divide and invade their environment. The growth rate of tumor cells is limited by the availability of oxygen (a field in our model), which cells consume from the environment. As oxygen gets depleted, tumor cells change their metabolic phenotype from “oxphos” to “glycolytic”. Glycolytic tumor cells can change

[1] Our choice is motivated by the methodological problems that surround the pre-clinical studies behind candidate (1) which make it less human-relevant than (2). See Discussion below.

phenotype back to "oxphos" if the oxygenation of the tissue is restored (i.e. the oxygen field strength increases). Otherwise, when oxygen is severely depleted, glycolytic cells become necrotic and die. Glycolytic cells and necrotic cells secrete lactate to the TME that serves as a recruiting signal for immune inhibitory cells (Tregs).

Our model includes two types of immune cells: Tcells (CTLs) and Tregs. Tcells can adopt one of two different phenotypes: "active" and "inactive". Inactive Tcells are constantly recruited to the tumor site and infiltrate the TME. Tcells are activated upon contact with tumor cells and induce apoptosis in the cancer cells they come into contact with. Upon activation, Tcells also release a cytokine signal to the TME ("INFγ" field), thus attracting other Tcells to their vicinity. The acidification of the TME by the glycolytic cells results in recruitment of Tregs to the tumor site. These newly recruited Tregs move through the tissue to areas of higher concentration of the lactate. Tregs inhibit active Tcells they come in close proximity to which turn the latter inactive.

We implemented the model in CompuCell3D (CC3D), an open-source modeling environment that allows specification and simulation of multicellular models, diffusing fields and biochemical networks [12]. CC3D simulates spatial dynamics using the Cellular Potts Model (CPM), a modeling framework where cells are represented on a lattice and their spatial properties are governed by an effective energy function (See *Supplementary Material*). Spatial dynamics are decided using a Monte Carlo approach, making each independent run stochastic, in which time is measured in Monte Carlo steps (MCS). Our model is simulated over $10^6$ lattice sites representing up to $5\times10^4$ individual cells. Diffusion solvers integrate partial differential equations describing the diffusion of oxygen, lactate, and cytokines across the whole simulation domain. The different outcomes of the simulation are dependent on the parameter values associated with aerobic fitness and with the emergent patterns of TME invasion associated with availability of resources and immune response.

**2.2. Parameters estimation.** Simulation parameters corresponding to the spatial properties of human solid tumor cells, transport of chemicals and rates of immune response were estimated from the literature. Each lattice site corresponds to $16\mu m^2$ such that the simulation domain represents a $16mm^2$ tissue cross section. We assumed that cancer cells occupy an area of $256\mu m^2$, which is between 2-3 times the average size of epithelial cells [13]. We assumed that when sufficient resources are available, tumor cells grow and divide every 24 hrs. Conversely, when resources are depleted cells die within 12 hrs, and when Tcells induce apoptosis cells die within 8 hrs. We estimated the infiltration rates of Tcells (1 cell every 1.5 hours) and Tregs (1 cell every 1 hour) using intramural density data, showing that the Tcell-Treg ratio is 5:1 [14].

The intrinsic random motility and the contact energy were fixed so that tumor cells can detach from each other and invade the surrounding tissue [6]. We assumed that the homeostatic concentration of oxygen in tissue is 4.3 M [15]. Transport parameters such as oxygen, lactate and INFγ diffusion coefficients, oxygen uptake rate and lactate secretion rate were estimated from the literature (See *Supplementary Material*). Aerobic fitness was defined as the oxygen

concentration threshold at which tumor cells changed from "oxphos" to "glycolytic". Different populations were defined with respect to different thresholds. The more aerobically fit a virtual subject is, the more tolerant its tissue will be to hypoxia, and as a result, the threshold for the shift from "oxphos" to "glycolytic" is lower.

**2.3. Sensitivity and robustness analysis.** We used Indiana University's large-memory computer cluster Carbonate to execute multiple replicates of the simulation [16]. Each replicate is intended to virtually represent individual cancer patient. To generate statistically meaningful results, 900 replicates representing individual patients across 9 aerobic fitness groups were simulated (100 replicates per group). Sensitivity analysis was performed by comparing simulation outcomes for different sets of parameters with respect to the final number of tumor cells per aerobic fitness group. The outcomes of the simulation are highly sensitive to key parameters such as the ratio of intratumoral Tcells/Treg, the maximum growth rate of tumor cells and the glycolytic threshold. Conversely, the outcomes are robust with respect to perturbation of parameters such as cell size or grid size.

### 2.4. Biological significance and calibration

#### 2.4.1. Mechanisms

**2.4.1.1. Glycolysis and hypoxia tolerance.** Ample studies point at elevated glycolysis as a hallmark of solid tumor progression [17,18]. To represent this biological feature in our model we introduced a lactate field, secreted by the tumor cells into the TME (**Figure 2**). According to our hypothesis, a solid tumor in aerobically fit (sedentary) hosts will generate weak (strong) lactate field depending on that host's tolerance to hypoxia. This hypothetical differential in turn drives the variation in immune response to the solid tumor.

**2.4.1.2. Tregs and Tcells dynamics.** Clinical studies have shown that intratumoral Treg/Tcell ratio is a significant prognostic marker for cancer patients [19] and several pre-clinical studies have tied this marker to hypoxic conditions in the TME [10,11]. To represent these biological features in our model we introduced two types of immune cells (CTLs and Tregs) and implemented two scales of trafficking (**Figure 3**). The first is the appearance of these cells in the TME, implemented with different "seeding" rates and densities; the second is movement within the TME, implemented with a chemotaxis mechanism. The seeding rates and densities were calibrated using data on respective densities from hot vs. cold tumors in humans [14]. The chemotaxis mechanisms are sensitive to two fields. CTLs react to a cytokine secreted by tumor cells killed by other CTLs (the "INFγ" field); Tregs react to the lactate field secreted into the TME (the more glycolytic is the tumor, the stronger is the Treg recruiting signal).

#### 2.4.2. Calibration

**2.4.2.1. Effect of aerobic fitness on tumor progression rate.** Our model connects variations in fitness levels to variations in anti-tumor immune response and consequently to variations in tumor growth rates. To calibrate it we used clinical results from breast cancer patients (where one could rely on hindsight and pre-diagnostic screening mammograms to estimate tumor growth rates with) [20]. The comparison yielded a classification of distinct aerobic fitness

levels, each of which yields a distinct tumor growth curve (**Figure 4**). A similar effect was shown qualitatively in pre-clinical studies [21,22].

**2.4.2.2. Distribution of tumor doubling time in the population.** Studies based on mammography readings [23] have discovered a distribution of tumor growth rates in the population (measured in tumor doubling times), which was shown to be lognormal. We ran a virtual experiment on our platform with 900 subjects divided uniformly into different aerobic fitness classes and compared the growth rate distribution to the one observed among humans. Both distributions (the virtual and the epidemiological) were lognormal (**Figure 5**).

**2.4.2.3. Prevalence of clinical tumors in athletes vs. non-athletes.** Finally, to identify the aerobically fit/sedentary divide in our model we used epidemiological studies on tumor incidence among athletes and non-athletes [3] (**Figure 6A**). The comparison allowed us to designate as "athletes" populations below 0.080, and sedentary above 0.140, were the fitness scales between 0.070 and 0.150, the lower the number the higher the aerobic fitness (**Figure 6B**). Lacking additional granularity of staging variations upon detection in both groups, we limited this calibration to the identification of a biologically significant spatiotemporal scale for the model: the incidence ratio observed in athletes and non athletes humans is achieved in our model for tumor size of 22000 cells and after 8000 MCS (equivalent to 35 days) (**Figure 6B**). Assuming a clinical (detectable) tumor threshold is $4mm^2$, we can use the incidence ratio to compare the scale of our virtual platform to clinical data: our simulated tumors will be detected when they reach a radius of 2mm (in the model), which is equivalent to real life tumors with radius of 3mm, or a scale of 3:2 (our simulation is the same order of magnitude of the real tumor). Additional data on the staging distribution upon detection in both groups could improve this calibration.

## 3. Results.

**3.1. Time series of anti-tumor immune response in the TME.** Our first virtual experiment probes the intricate dynamics in the TME between the tumor and the infiltrating immune cells. Such dynamics is impossible to probe in humans, is hard to observe during a pre-clinical study as it requires significant of redundancy in lab animals (as to achieve high resolution with statistical significance for successive end-points during the experiment), prohibiting such time and labor intensive studies. Our simulation generates, with no physical cost, a time series of spatiotemporal snapshots of the TME (**Figure 7**) that can serve as a platform to test several mechanistic hypotheses on the role and dynamics of different immune cells in ant-tumor immune response, by comparing it to immunohistochemistry slides from different stages of tumor development. While here we focused only on two types of immune cells (CTLs and Tegs), and two types of signaling fields (INFγ and lactate), the platform is modular and can incorporate many more cells and fields with relatively small modifications.

**3.2. Incorporating aerobic fitness into the personalization of immunotherapy.** While showing remarkable success in some patients, immunotherapy treatments can lead to severe autoimmune adverse effects such as myocarditis, pericardial diseases, and vasculitis, including temporal-arteritis and vision loss [5]. To mitigate those, careful dosing is essential. If our hypothesis is correct (and there is some support for it from pre-clinical studies on the

combination of Immune Checkpoint Inhibitors (ICI) with aerobic exercise [22] and from small pre-treatment exercise intervention in humans [24]), aerobically fit patients may require smaller dosage of ICI than sedentary patients, which may lead to personalization of treatment and reduction of adverse effects. To test this hypothesis we implemented ICI in our model as an increased efficacy of CTL killing, by enlarging the killing radius of each CTL. Cytotoxicity was then modeled with an additional cytokine field, where the probability of an adverse effect [25] increases with that field's strength. Performing a virtual experiment on both aerobically fit and sedentary subject populations treated with ICI, the model shows how, without a mitigated dosage, aerobically fit subjects are more prone to adverse effects than their sedentary counterparts (**Figure 8A,B**). Conversely, lowering the dosage of ICI for aerobically fit patients can achieve the same reduction of tumor growth relative to their sedentary counterparts but with a lower probability for adverse effects (**Figure 8C,D**).

## 4. Discussion.

**4.1. What we have shown**. After calibrating our model with clinical and epidemiological data, we performed two virtual experiments that showcase the potential usefulness of the platform as a tool for improving pre-clinical and clinical studies. We have shown how to generate a time series of TME snapshots during anti-tumor immune response, and how to personalize dosing of ICI for aerobically fit patients in order to lower the risk of adverse effects.

**4.2. Justification.** Why exercise? Because it has been shown to be a systemic modulator of metabolic and endocrinal activities, and, through these, a modulator of immune competence, and a natural element in cancer prevention, and, as we suggest here, cancer (immuno)therapy.

The exact underlying mechanisms behind the suppressive effects of aerobic exercise on early tumor progression are currently unknown. Several pre-clinical studies have narrowed the possibility space down to two main hypotheses. The first involves exercise-induced up-regulation of epinephrine that mobilizes NK cells into the TME [7,8] together with increased trans-signaling of IL-6 [26,27] as a re-distributing factor (increased adhesion, infiltration and activation). However, since these effects were induced on mice by exposing them to voluntary running, their human relevance is suspect [28]: voluntary running in mice mimics high intensity interval training (HIIT) in humans, and no human, even an elite athlete, can endure the "dosage" level of HIIT exhibited in those studies [29,30]. Since there are currently no experiments testing this hypothesis with more human-relevant, lower HIIT "dosage" (in which the voluntary wheel is activated only for a short period per day), and since our goal here is practical, our model focuses on the second candidate whose human-relevance is more significant.

This second hypothesis, the one we focused on here, connects exercise-induced increased hypoxia-tolerance to more efficient anti-tumor immune response, and requires chronic endurance training (CET) which can be achieved in pre-clinical exercise oncology with forced running wheels [21,28]. The idea here is that CET induces hypoxia tolerance in the skeletal muscles and in other tissues, and as a result TMEs are more susceptible to the degradation of HIF1α [31]. This degradation is an upstream factor in a signaling cascade leading to increased anti-tumor immune efficiency, as HIF1α is known to recruit, via myokine signaling [10,11,32], Trges into the tumor micro-environment, which suppress CTLs [9,21]. Support for this

potential mechanism in humans that connects CET with reduced intratumoral Treg density comes from a small pilot study in which recently diagnosed breast cancer patients were subject to a short exercise session before treatment, and their excised tumor presented with fewer intratumoral Tregs [24].

**4.3. Limitations.** Our platform can perform virtual experiments with no wet-lab costs, and is proposed here as a tool for pre-clinical and clinical researchers. The tool is limited in several ways. First, to obtain simulation results in a reasonable time we must limit the computational cost. Consequently, our grid size is currently bounded by $5\times10^4$ cells. This size allows the simulation to be sensitive to spatiotemporal and stochastic features of the dynamics; increasing it will incur computational cost, but given the running time of the current simulation, shouldn't be prohibitive. Second, the same concerns about computational cost limit us to two-dimensional simulations. Specific circumstances may require scaling up to 3D (e.g., angiogenesis), which can be done on segments of the grid to reduce complexity. For most clinical end-points, however, a cross section of the TME may be a good approximation. Third, here we introduced only two types of immune cells and three types of fields. Increasing the number of members of both sets will, again, add complexity (and computational cost) to the model. From our experience, however, a direct dialogue between model developers and clinicians may help optimize the platform for each specific usage so that the computational cost won't become prohibitive. Finally, note that we deliberately calibrated the model solely with quantitative clinical and epidemiological data, and limited the usage of pre-clinical studies to qualitatively probing mechanistic hypotheses. We did so because our platform faces a challenge prevalent in biomedical research in general, namely, spatiotemporal scaling between mice models and human models. Acknowledging this challenge, we believe we are better equipped to meet it: once the model is separately calibrated for each modality, it allows us to virtually compare time series from pre-clinical simulations to observed clinical end-points (a process that is hard to mimic in real-life experiments) and help to characterize the scaling between murine and human immunological clocks.

**4.4. Insights and future directions.** Solid tumor progression is an intricate process that can be characterized with population dynamics where tumor cells and immune cells are intertwined in complex signaling networks. As such it is sensitive to spatiotemporal factors which are difficult to incorporate into current machine-learning-based bioinformatics platforms. Causal multi-scale modeling is a viable alternative that can mitigate this shortcoming; our *in-silico* modeling platform of anti-tumor immune response and early stage solid tumor growth presented here is an example. The long-term goal of all such modeling, which can only show that a specific underlying mechanism is *sufficient* to explain the observed phenomena, is the development of quantitative, predictive models based on clinical and experimental data which will have a positive impact on patient outcomes through improved patient-specific treatment regimes.

Perhaps more than any other therapy, cancer immunotherapy is particularly sensitive to timing [33]. Efforts invested in examination of combination dose scheduling can yield qualitatively significant returns in terms of improved efficacy and decreased toxicity; all without necessitating regulatory approval. Our *in silico* platform is a safe playground for such experimentation in dosage scheduling and frequency, as it can easily allow modulation of duration and timing of activation signaling to achieve the most effective treatment, thus ruling

out extreme scenarios and refocusing the researcher on an optimal treatment window, and harmlessly test different dosage regimes and duration.

Finally, our platform can easily incorporate and test combination of different types of immunotherapy with other standard-of-care therapies [34] and probe potential synergistic effects. For example, since aerobic exercise promotes oxygenation, it can mimic the effects of Anti Angiogenic Therapy (AAT), where different aerobic fitness levels can be calibrated to represent different dosage of such a therapy.

Here we presented a small sample what the platform can offer. To fully achieve its potential, it requires careful calibration with clinical data and cross talk with pre-clinical experimental set-ups. To this end, we hope to start a dialogue with interested cancer immunotherapy clinicians and pre-clinical researchers who are open to incorporating *in silico* modeling into their experimental portfolio.

**Abbreviations**

| | |
|---|---|
| **AAT** | anti angiogenic therapy |
| **CC3D** | CompuCell 3D |
| **CET** | chronic endurance training |
| **CPM** | cellular Potts model |
| **CTL** | cytotoxic T lymphocytes |
| **HIIT** | high intensity interval training |
| **ICI** | immune checkpoint inhibitors |
| **MCS** | Monte Carlo steps |
| **TME** | tumor microenvironment |

**Declarations.**

**Funding** This research was supported in part by Lilly Endowment, Inc., through its support for the Indiana University Pervasive Technology Institute.

**Conflicts of interest/Competing interests** AH is the inventor and owner of US patent 10.497.467.B2 Systems and Methods for Optimizing Diagnostics and Therapeutics with Metabolic Profiling

**Ethics approval** N/A

**Consent to participate** N/A

**Consent for publication** N/A

**Availability of data and material** All data was retrieved from published literature at PUBMED

**Code availability** Code is available from JAS upon request

**Authors' contributions** Conceptualization: AH. Model conceptualization: AH & JAS. Coding and Running Simulations: JAS; Manuscript writing and editing: AH & JAS.

**Acknowledgments** The authors acknowledge the Indiana University Pervasive Technology Institute for providing HPC (Carbonate) resources that have contributed to the research results reported here. URL: https://pti.iu.edu/. We thank James Glazier (IUB) for useful discussion. AH thanks Guilherme Oliveira for earlier work on this project.

**Bibliography**

1. Ashcraft KA et al (2016). Efficacy and mechanisms of aerobic exercise on cancer initiation, progression, and metastasis: A critical systematic review of *in vivo* preclinical data. Cancer Research 76(14): 4032–4050. https://doi.org/10.1158/0008-5472.CAN-16-0887

2. Betof AS. et al (2015). Modulation of murine breast tumor vascularity, hypoxia, and chemotherapeutic response by exercise. J Natl Cancer Inst. 107(5): 1-5. [PMID: 25780062]

3. Frisch R. et al (1985). Lower prevalence of breast cancer and cancers of the reproductive system among former college athletes compared to non-athletes. British Journal of Cancer 52: 885-891. [PMID: 4074640]; and Frisch R, Wyshak G. Breast cancer among former college athletes compared to non-athletes: a 15-year follow-up. British Journal of Cancer 82(3): 726-30. [PMID: 10682689]

4. Friedenreich CM (2011). Physical activity and breast cancer: review of the epidemiologic evidence and biologic mechanisms. Recent Results in Cancer Research 188: 125-39. [PMID: 21253795]

5. Salem J. et al (2018). Spectrum of cardiovascular toxicities of immune checkpoint inhibitors: A pharmacovigilance study. Lancet Oncol. 19(12): 1579–1589. https://doi:10.1016/S1470-2045(18)30608-9

6. Swat M. et al (2015). Emergent stratification in solid tumors selects for reduced cohesion of tumor cells: A multi-cell, virtual-tissue model of tumor evolution using *CompuCell3D*. PLoS ONE 2015;10(6): e0127972. [PMID: 26083246]

7. Hojman P et al (2011). Exercise-induced muscle-derived cytokines inhibit mammary cancer cell growth. Am. J. Physiol. Endocrinol. Metab. 301, E504– E510. https://doi.org/10.1152/ajpendo.00520.2010

8. Pedersen L et al (2016). Voluntary Running Suppresses Tumor Growth through Epinephrine- and IL-6-Dependent NK Cell Mobilization and Redistribution. Cell Metabolism 23, 1–9. http://dx.doi.org/10.1016/j.cmet.2016.01.011

9. Lee CT, Mace T, Repasky EA (2010). Hypoxia-driven immunosuppression: a new reason to use thermal therapy in the treatment of cancer? Int J Hyperthermia. 26(3):232–246 doi: 10.3109/02656731003601745

10. Tumor hypoxia promotes tolerance and angiogenesis via CCL28 and T(reg) cells Nature 475(7355): 226–230 [PMID 21753853]

11. Ren L et al (2016). Hypoxia-induced CCL28 promotes recruitment of regulatory T cells and tumor growth in liver cancer. Oncotarget 7(46):75763-73 [PMID 27712661]

12. Swat MH et al (2012). Multi-scale modeling of tissues using CompuCell3D. Methods Cell Biol. 110: 325–366. doi:10.1016/B978-0-12-388403-9.00013-8

13. Mendelsohn J. et al (2015) The Molecular Basis of Cancer. Sounders, USA, pp. 274

14. 15. Kather JN et al (2018). Topography of cancer-associated immune cells in human solid tumors. *eLife 7*: e36967. https://doi.org/10.7554/eLife.36967

15. Casciari JJ et al (1992). Variations in tumor cell growth rates and metabolism with oxygen concentration, glucose concentration, and extracellular pH. Journal of Cellular Physiology 151(2): 386-394

16. Stewart CA et al (2017). Indiana University Pervasive Technology Institute. Bloomington, IN. https://doi.org/10.5967/K8G44NGB

17. Pavlova NN, Thompson CB (2016). The Emerging Hallmarks of Cancer Metabolism. Cell Metab. 23(1):27–47. https://doi:10.1016/j.cmet.2015.12.006

18. Semenza GL (2016). The hypoxic tumor microenvironment: A driving force for breast cancer progression. Biochimica et Biophysica Acta 1863(3): 382-391 https://doi.org/10.1016/j.bbamcr.2015.05.036

19. Shitara, K. and Nishikawa, H. (2018), Regulatory T cells: a potential target in cancer immunotherapy. Ann. N.Y. Acad. Sci., 1417: 104-115. doi:10.1111/nyas.13625

20. Hagar A et al (2018). Muscular endurance and progression rates of early-stage invasive ductal carcinoma: A pilot study. Breast J 24(5): 849-851

21. Hagar A et al (2019). Endurance training slows breast tumor growth in mice by suppressing Treg cells recruitment to tumors. BMC cancer 19(1): 536. https://doi.org/10.1186/s12885-019-5745-7

22. Wennerberg E et al (2020). Exercise reduces immune suppression and breast cancer progression in a preclinical model. Oncotarget 11(4):452-461

23. Spratt J. et al (1993). Mammographic assessment of human breast cancer growth and duration. Cancer. 71(6): 2020-6 https://doi.org/10.1002/1097-0142(19930315)71:6<2020::aid-cncr2820710616>3.0.co;2-#

24. Ligibel JA, Dillon D, Giobbie-Hurder A et al (2019). Impact of a pre-operative exercise intervention on breast cancer proliferation and gene expression: results from the pre-operative health and body (PreHAB) study. Clin Cancer Res. 25(17): 5398-5406. [PMID: 31018921]

25. Postow MA, Sidlow R, Hellmann MD. (2018). Immune-related adverse events associated with immune checkpoint blockade. NEJM 378(2): 158-168. https://doi:10.1056/NEJMra1703481

26. Rose-John S. (2012). IL-6 trans-signaling via the soluble IL-6 receptor: Importance for the pro-inflammatory activities of IL-6. *Int. J. Biol. Sci.* **8:** 1237-1247 [PMID: 23136552]

27. Evans S. et al (2001). Fever-range hyperthermia dynamically regulates lymphocyte delivery to high endothelial venules. *Blood* **97:** 2727-33 [PMID: 11313264]

28. Melo L, Hagar A. (2019). How to train a mouse. *Am J Cancer Res* 9(6): 1246-1253 [PMID: 31285956]

29. Seiler S, Tønnessen E. (2009). Intervals, thresholds, and long slow distance: the role of intensity and duration in endurance training. Sport Science 13: 32-53 https://www.sportsci.org/2009/ss.htm

30. Stöggl TL, Sperlich B. (2015). The training intensity distribution among well-trained and elite endurance athletes. *Frontiers in physiology*, *6*, 295 https://doi.org/10.3389/fphys.2015.00295

31. Petrova V, Annicchiarico-Petruzzelli M, Melino G, Amelio I. The hypoxic tumour microenvironment. *Oncogenesis*. 2018;7(1):10. https://doi.org/10.1038/s41389-017-0011-9

32. Ben-Shoshan J et al (2008), Hypoxia controls $CD4^{+}CD25^{+}$ regulatory T-cell homeostasis *via* HIF1α. Eur. J. Immunol. 38: 2412-2418. https://doi:10.1002/eji.200838318

33. Rothschilds AM, Wittrup KD (2019) What, Why, Where, and When: Bringing Timing to Immuno-Oncology. Trends in Immunology. 40(1): 12-21. https://doi.org/10.1016/j.it.2018.11.003

34. Andersson P, Ostheimer C (2019) Editorial: Combinatorial Approaches to Enhance Anti-tumor Immunity: Focus on Immune Checkpoint Blockade Therapy. Frontiers in Immunology. 10:2083. https://doi.org/10.3389/fimmu.2019.02083

**Figures Captions**

1. **Model Conceptualization.** The model simulates the early stage of solid tumor progression from which a growth rate can be calculated. Once initialized, tumor cells grow in the TME, and with time become more glycolytic, in a rate that depends on the host's aerobic fitness and tolerance to hypoxia. Tumor cells die through apoptosis or necrosis (lack of oxygen or death by CTLs). CTLs and Tregs react to cytokine and lactate fields secreted by tumor cells. Tumor cells grow until they saturate the grid.

2. **Aerobic fitness modulates hypoxia-tolerance in the TME.** The more aerobically fit is the host (FIT), the more tolerant to hypoxia its TME is, and as a result tumor cells are less glycolytic relative to sedentary hosts (SED).

3. **Aerobic fitness modulates anti-tumor immune response.** The more aerobically fit is the host, the less glycolytic its tumor cells are relative to a sedentary host. Consequently, recruitment of Trges that can block CTLs is down regulated relative to a sedentary host, and tumor growth will be relatively suppressed (3A,B). Tregs move towards the tumor along the lactate gradient that glycolytic tumor cells secrete (3C). CTLs move towards the tumor along a cytokine gradient ("INFγ") that necrotic tumor cells secrete (3D). Once infiltrated into the TME, they can block the ability of nearby CTLs to kill tumor cells.

4. **Effect of aerobic fitness on tumor progression rate**. The model was run on 900 virtual subjects, divided into equal size distinct aerobic fitness levels. Each fitness level generated an average growth rate (4A). These average growth rates where then plotted against the fitness levels on a logarithmic scale (4B). The model behaves qualitatively in accordance with a similar plot of tumor doubling times vs. fitness levels from a pilot study in recently diagnosed T1 invasive ductal carcinoma patients (4C) [20].

5. **Distribution of tumor doubling time in the population.** We ran the model with 900 subjects with random fitness levels. The statistical distribution of growth rates (5A,B) was statistically indistinguishable in a KS test ($p>0.15$) from an observed log normal distribution of growth rates of invasive ductal carcinoma (5C, [23]).

6. **Prevalence of clinical tumors in athletes vs. non-athletes.** Epidemiological data shows prevalence of solid tumors in non-athletes to be around twice the prevalence in athletes (6A) [3]. We used this data point to extract a spatiotemporal calibration of the model by running 400 subjects, aerobically fit and sedentary, and identifying the tumor size (in number of model cells) and the time after initiation (in model time steps MCS) in which such a prevalence ratio is achieved (6B).

7. **Time series of TME sections in early stage progression of a solid tumor.** To probe the intricate dynamics of anti-tumor immune response in the early stages of a solid tumor progression, the model can yield an observation window into the TME in different stages of growth (7A-D), and can be used to test competing hypotheses on tumor immune cells population dynamics by comparing these snapshots to real life

immunohistochemistry (7E, [21]), where cross sections from exercised ("FIT") and sedentary ("SED") mice show different intratumoral $CD8^+/FOXP3^+$ ratios.

8. **Precision immunotherapy.** Aerobically fit patients may require smaller dosage of ICI than sedentary patients, which may lead to personalization of treatment and reduction of adverse effects. Without a mitigated dosage, aerobically fit subjects are more prone to adverse effects than their sedentary counterparts (8A,B). Lowering the dosage of ICI for aerobically fit patients can achieve the same reduction of tumor growth relative to their sedentary counterparts (8C) but with a lower probability for adverse effects (8D). 8E and 8F show tumor treated with high and low dosage of ICI, respectively.

Fig. 1

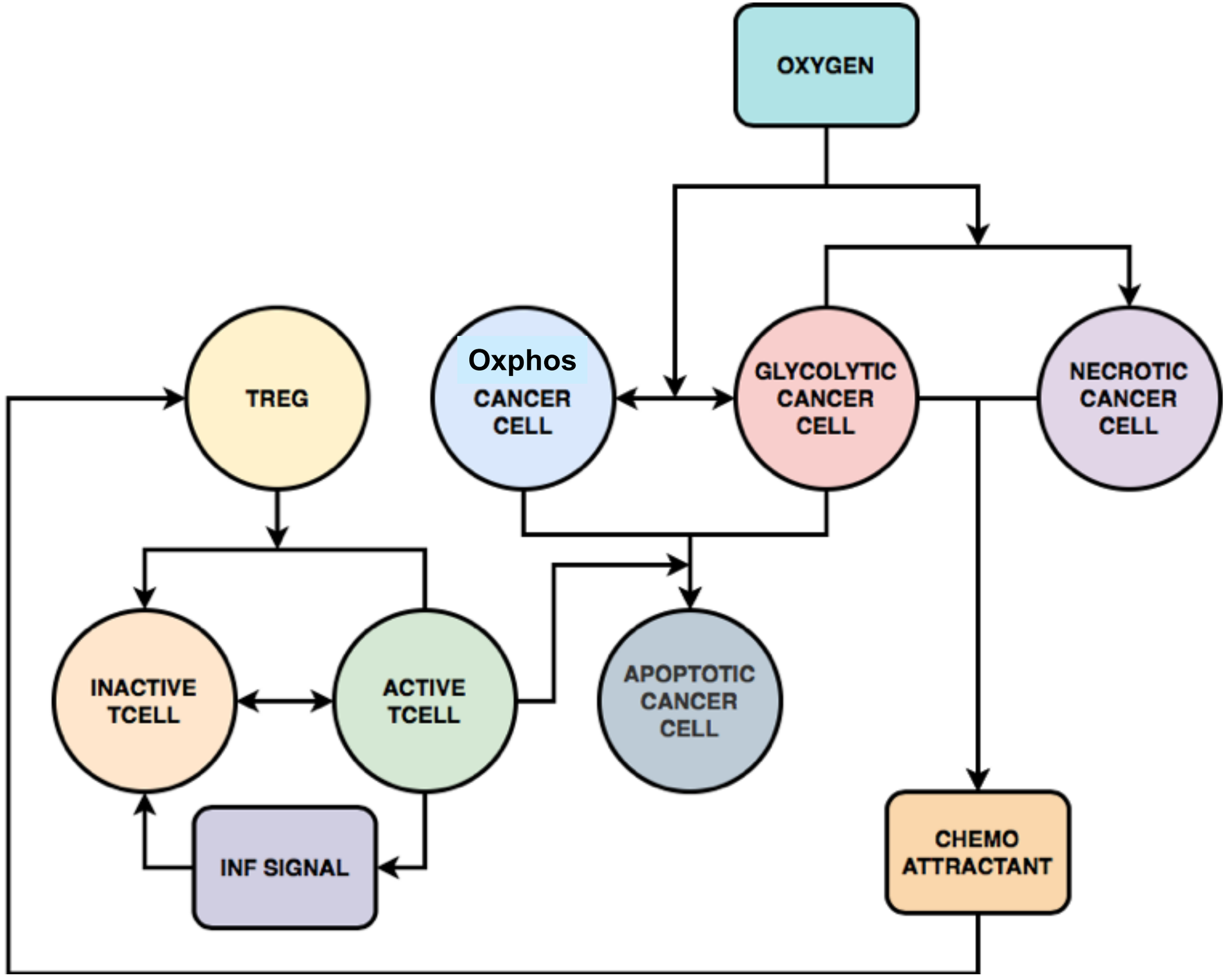
OXYGEN
TREG
Oxphos
CANCER
CELL
GLYCOLYTIC
CANCER
CELL
NECROTIC
CANCER
CELL
INACTIVE
TCELL
ACTIVE
TCELL
APOPTOTIC
CANCER
CELL
INF SIGNAL
CHEMO
ATTRACTANT

Fig. 2

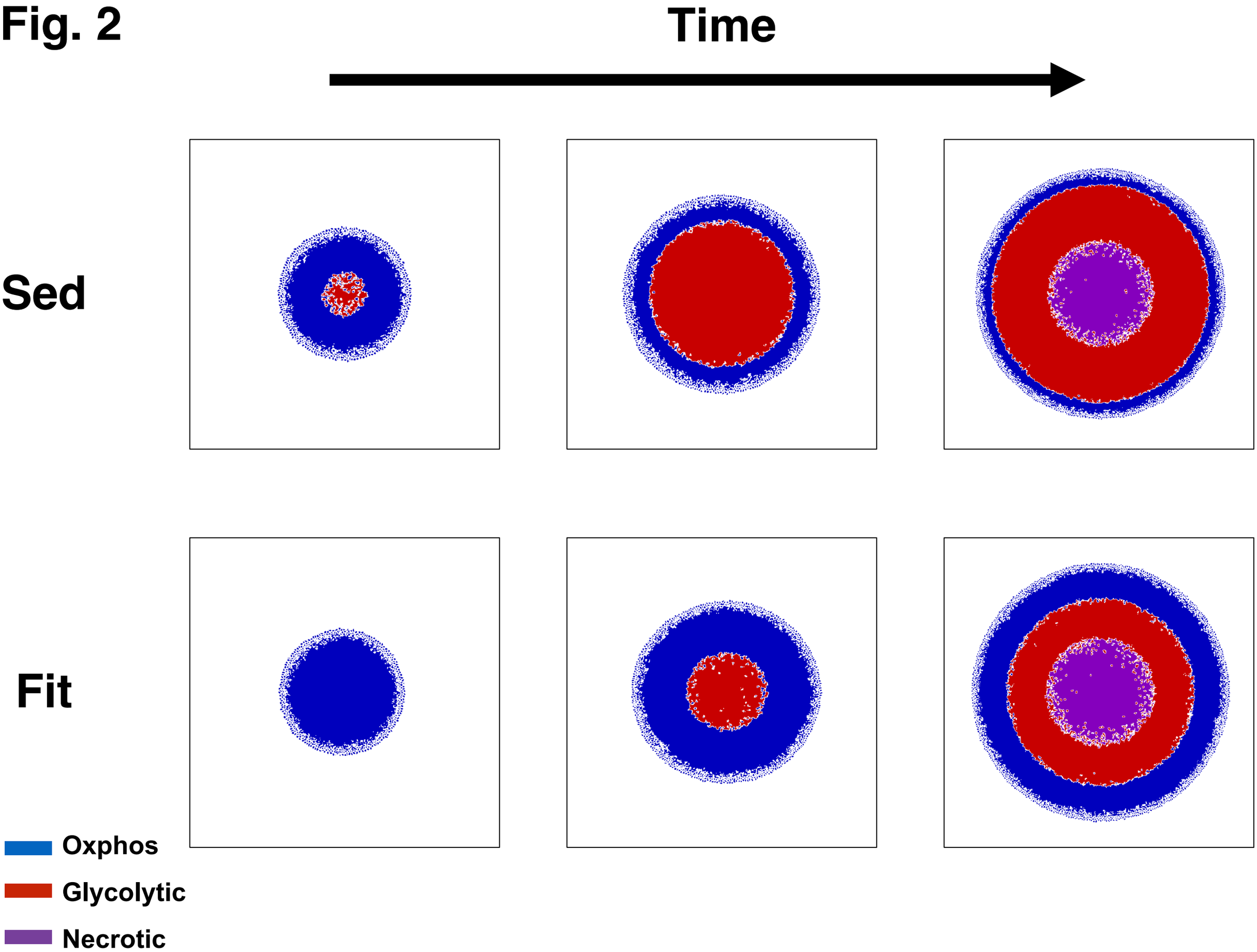

# Fig. 3

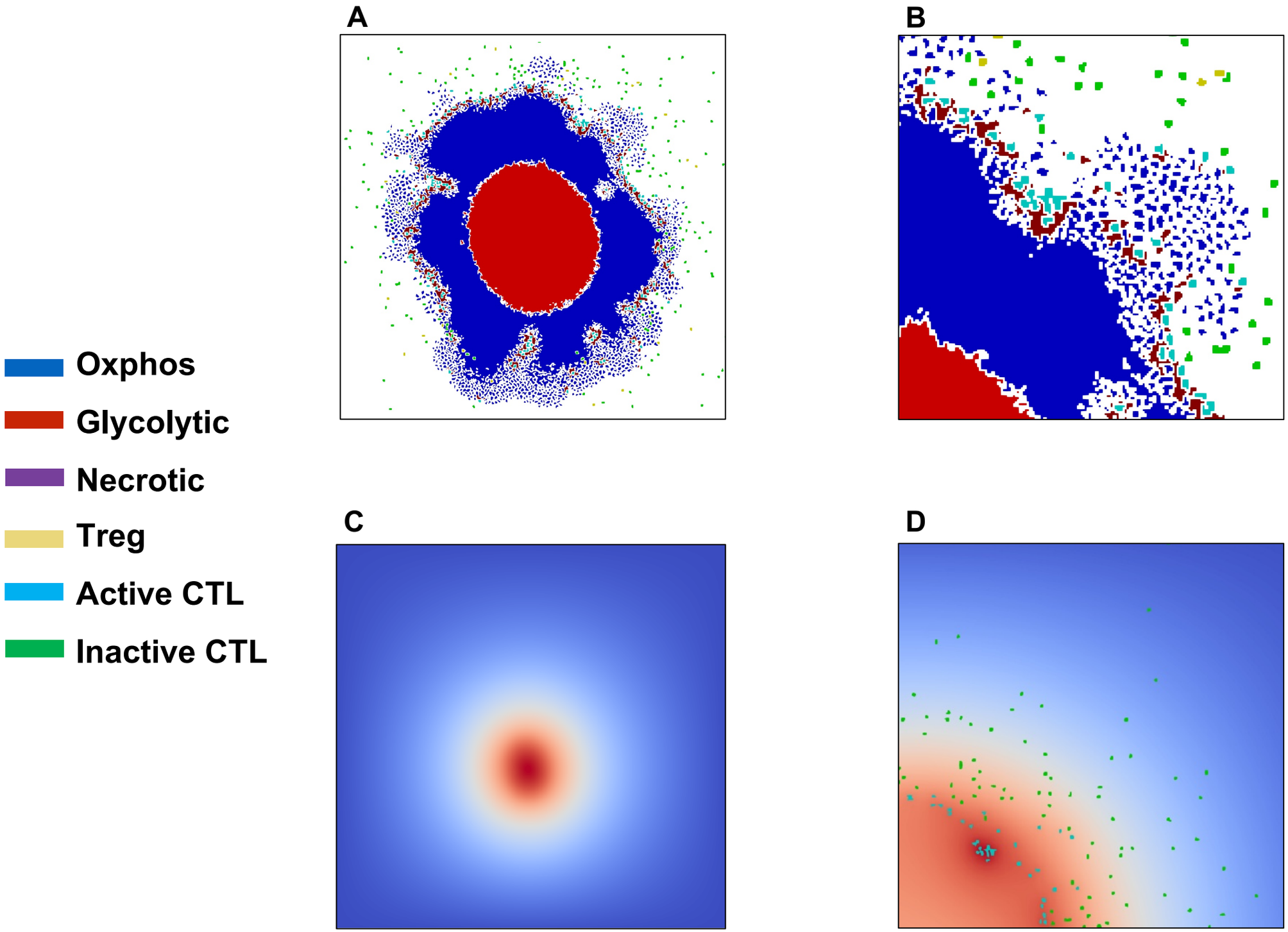
A
B
C
D
Oxphos
Glycolytic
Necrotic
Treg
Active CTL
Inactive CTL

# Fig. 4

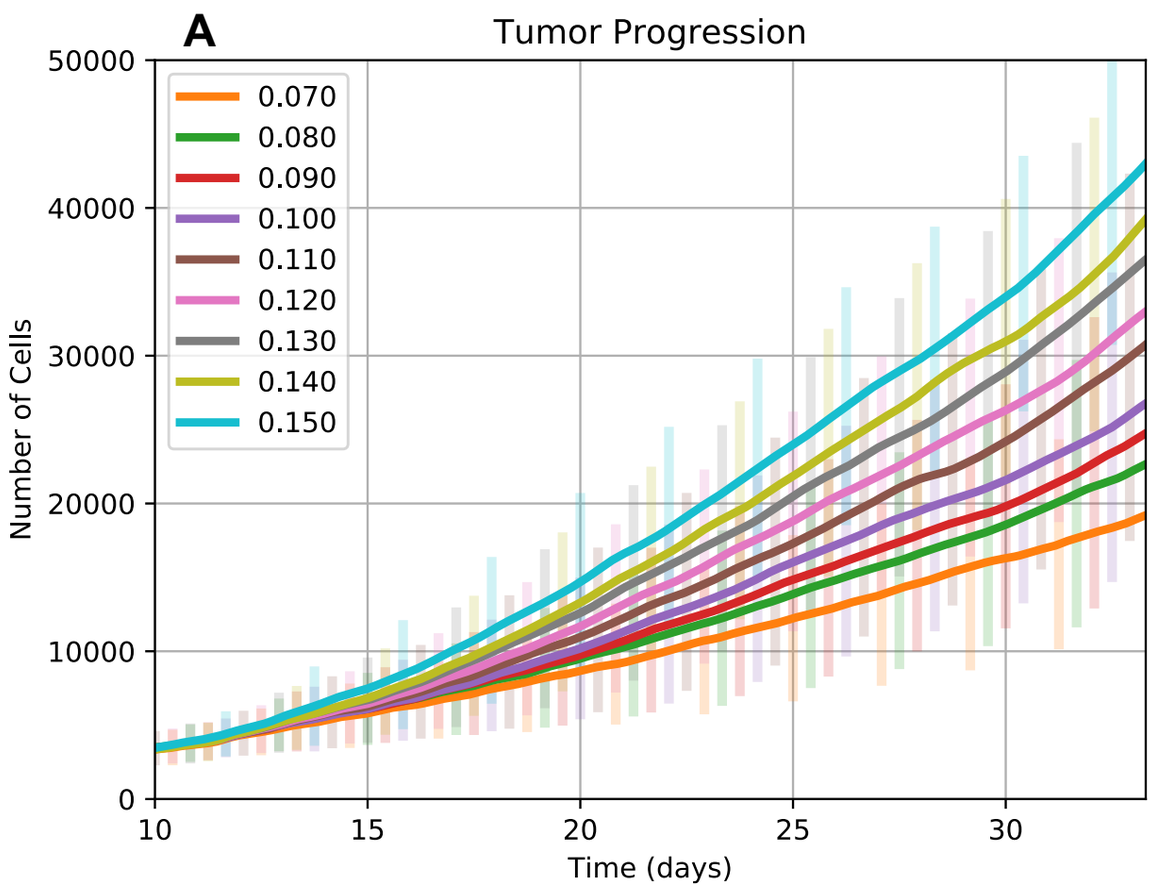
A
Tumor Progression
0.070
0.080
0.090
0.100
0.110
0.120
0.130
0.140
0.150
Number of Cells
Time (days)
0
10000
20000
30000
40000
50000
10
15
20
25
30

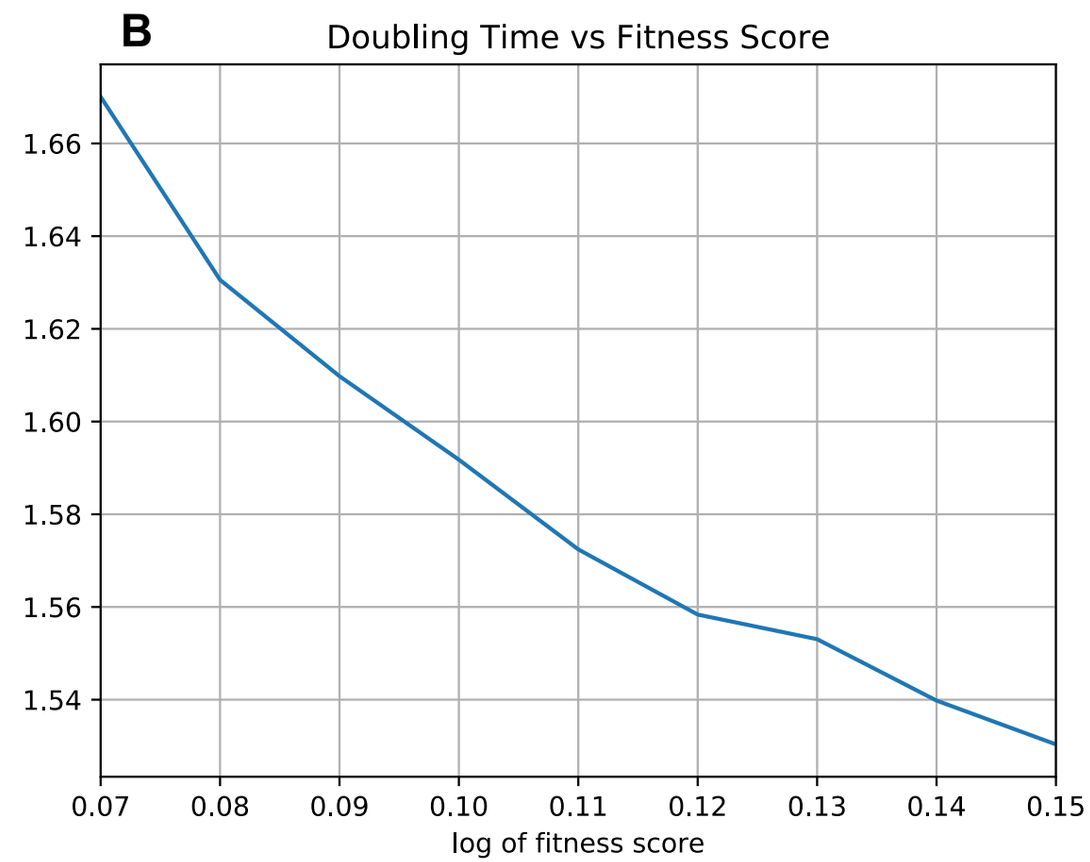
B
Doubling Time vs Fitness Score
log of fitness score
1.54
1.56
1.58
1.60
1.62
1.64
1.66
0.07
0.08
0.09
0.10
0.11
0.12
0.13
0.14
0.15

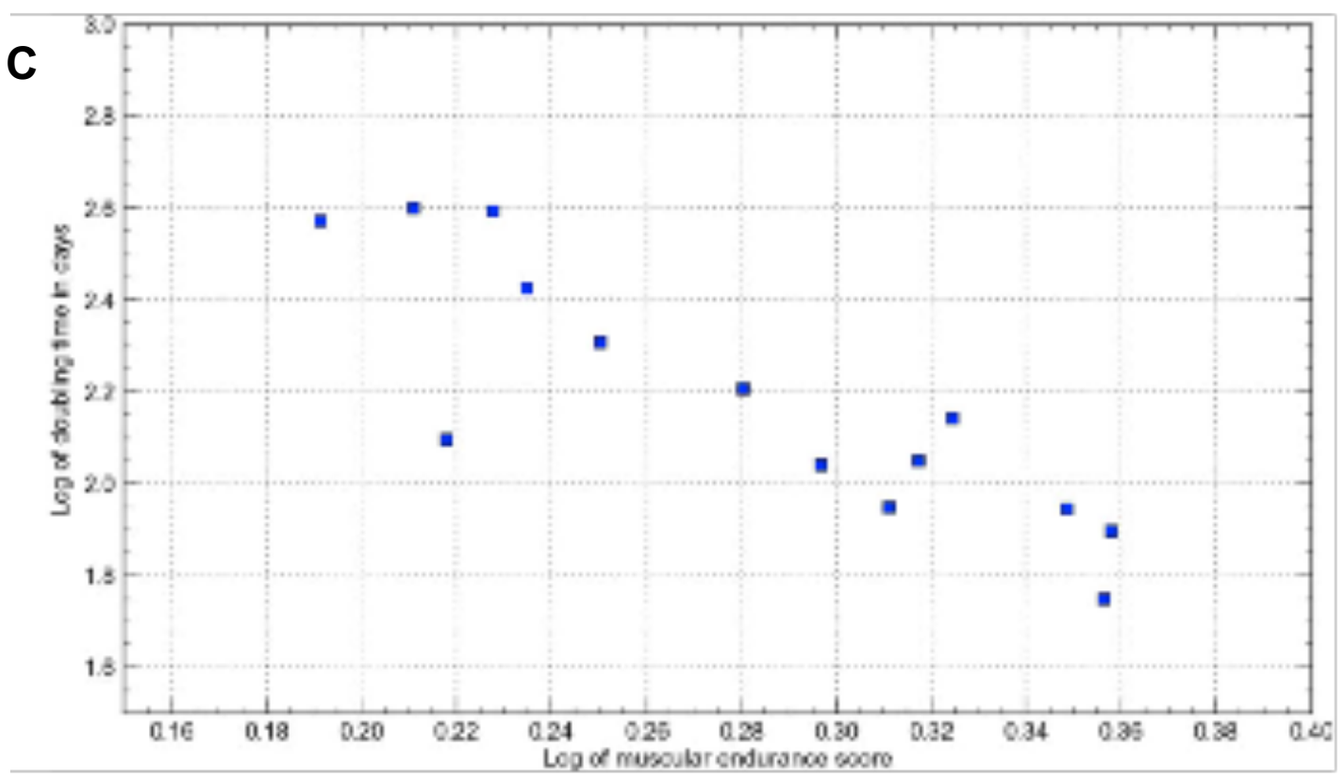
C
Log of doubling time in days
Log of muscular endurance score
1.6
1.8
2.0
2.2
2.4
2.6
2.8
3.0
0.16
0.18
0.20
0.22
0.24
0.26
0.28
0.30
0.32
0.34
0.36
0.38
0.40

# Fig. 5

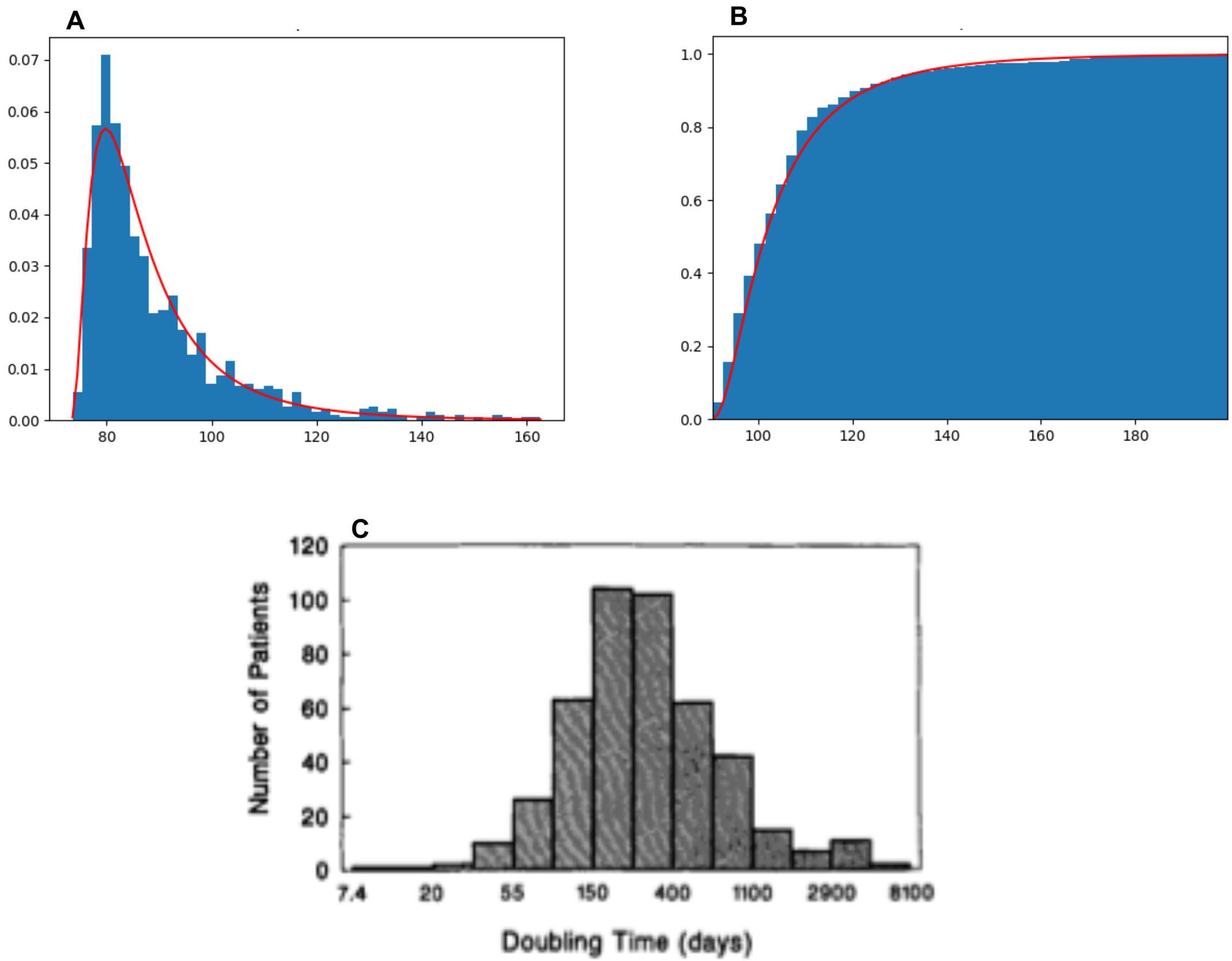
A
0.07
0.06
0.05
0.04
0.03
0.02
0.01
0.00
80
100
120
140
160
B
1.0
0.8
0.6
0.4
0.2
0.0
100
120
140
160
180
C
120
100
80
60
40
20
0
Number of Patients
7.4
20
55
150
400
1100
2900
8100
Doubling Time (days)

# Fig. 6

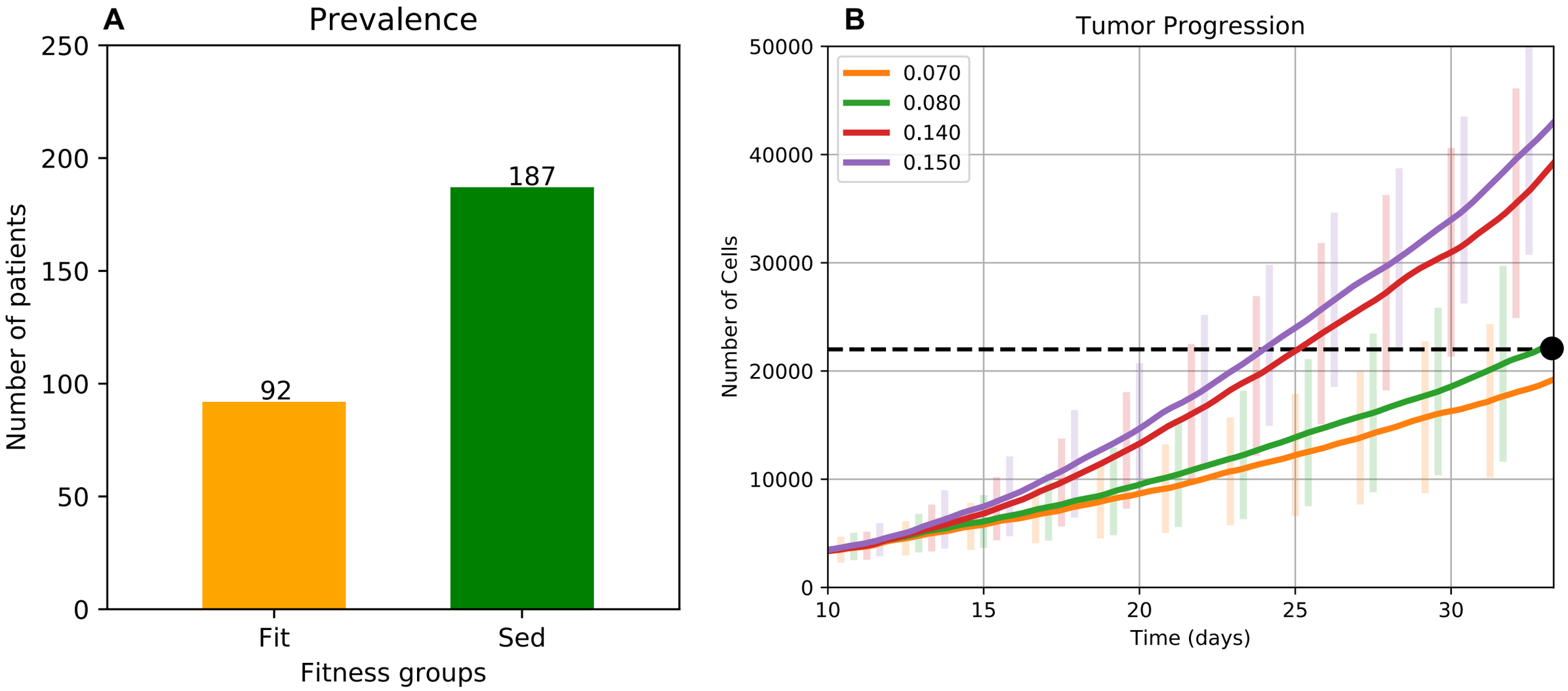
A
Prevalence
250
200
150
100
50
0
Number of patients
187
92
Fit
Sed
Fitness groups
B
Tumor Progression
50000
40000
30000
20000
10000
0
Number of Cells
0.070
0.080
0.140
0.150
10
15
20
25
30
Time (days)

# Fig. 7

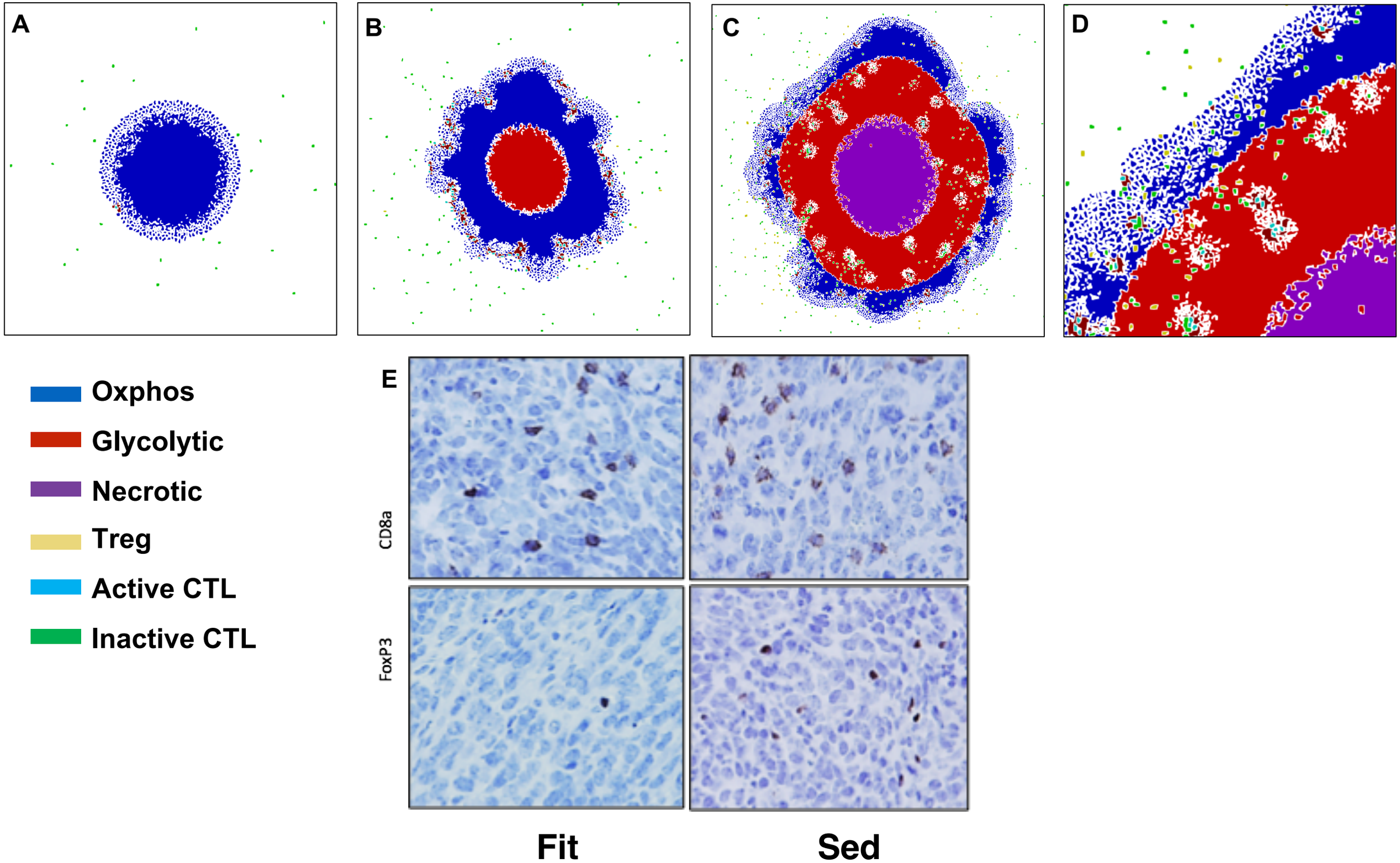
A
B
C
D
Oxphos
Glycolytic
Necrotic
Treg
Active CTL
Inactive CTL
E
CD8a
FoxP3
Fit
Sed

# Fig. 8

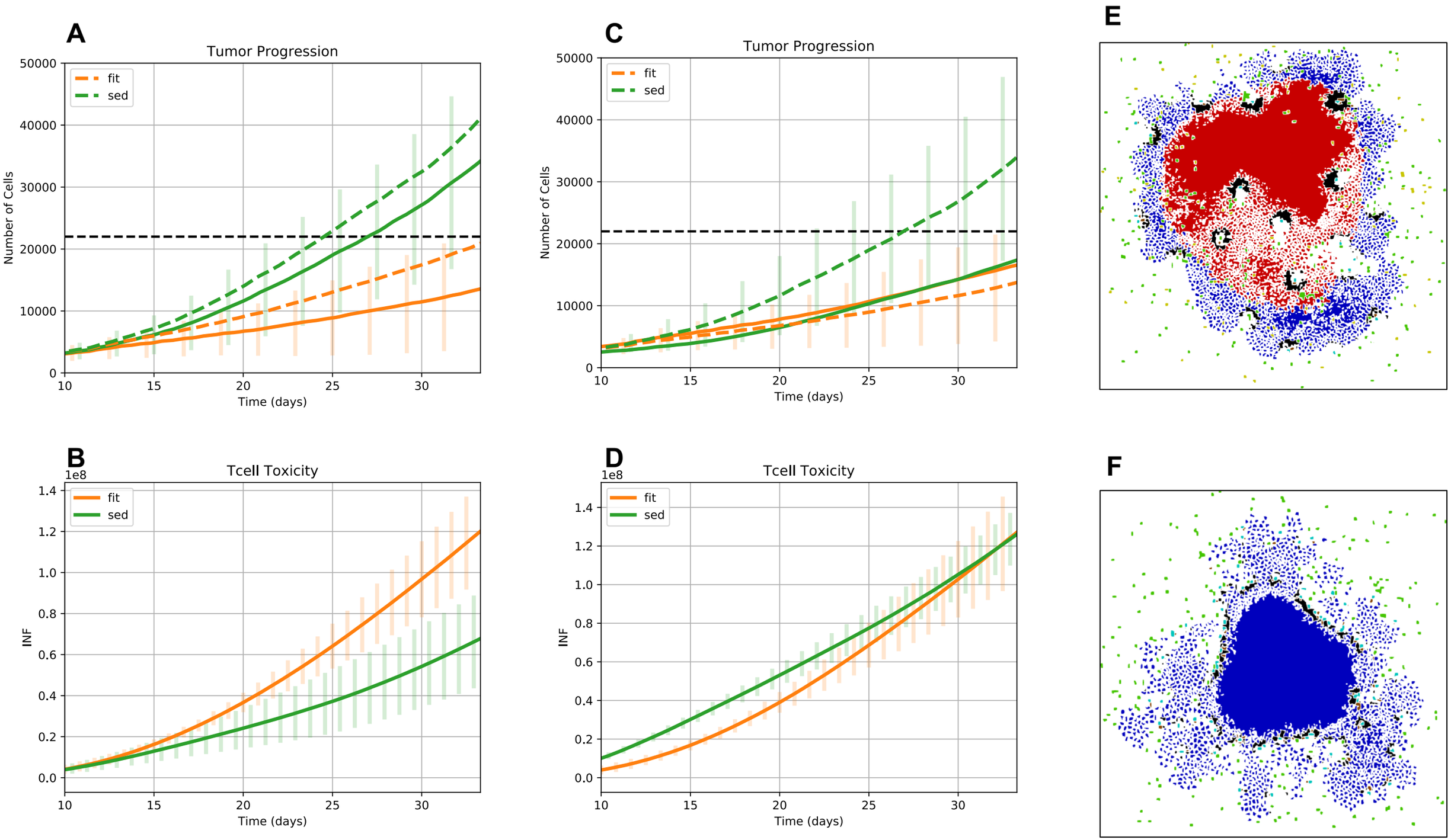
A
Tumor Progression
fit
sed
Number of Cells
Time (days)
B
Tcell Toxicity
1e8
INF
C
D
E
F